Calculation of the efficiency of polarization-insensitive surface-stabilized ferroelectric liquid-crystal diffraction gratings

Carl V. Brown and Emmanouil E. Kriezis

A rigorous analysis is presented of the diffraction efficiency of a polarization-insensitive surface-stabilized ferroelectric liquid-crystal (SSFLC) phase grating, taking full account of the internal structure of the ferroelectric liquid-crystal layer. When no field is applied, the twisted director profile in the relaxed state gives an optimum diffraction efficiency for a device thickness between the half-wave-plate and the full-wave-plate conditions. The influence of the magnitude of the spontaneous polarization and applied ac fields are investigated, and it is shown that the diffraction efficiency of a binary SSFLC phase grating can be strongly enhanced with the technique of ac stabilization. © 2003 Optical Society of America

OCIS codes: 050.1950, 160.3710, 200.4650, 260.1180.

1. Introduction

Ferroelectric liquid-crystal (FLC) diffraction grating devices have been utilized in optical computing systems,[1–3] as optical routing components in telecommunication systems,[4,5] and also as optical memories in three-dimensional holographic display systems.[6] The desirable properties of FLC spatial light modulators in these applications include their bistability, their fast switching times, and, particularly important, their ability to operate in a polarization-insensitive mode.[7,8] The third property means that high diffraction efficiencies are possible, irrespective of the incoming light polarization, and this property significantly reduces overall system losses when operation over unpredictable incoming polarizations (such as in optical communication systems) is expected.

The modeling of phase-modulation FLC devices generally assumes that the FLC device acts as a uniform switchable birefringent wave plate with no internal structure. In this case the diffraction efficiency is determined by the dimensionless parameter $\Delta nd/\lambda$ and the in-plane switching angle 2β between the optical axes of the two bistable states. Here Δn is the difference in refractive indices parallel and perpendicular to the optical axis, d is the thickness of the FLC layer, and λ is the free-space wavelength of incident light. The angle β is related to the smectic cone angle θ of the FLC material with the maximum efficiency occurring for $\beta = 45°$.[7–9] For this reason, materials such as CS2005 and CDRR8, which have a high cone angle and a first-order transition from isotropic to smectic C* phase, are often utilized in phase-modulation devices.[10–12]

The surface-stabilized FLC (SSFLC) geometry is based on materials that show an isotropic–nematic–smectic A–smectic C* phase sequence.[13] This geometry has also been used in phase-modulation mode devices[9,14] as well as displays and spatial light modulators based on amplitude modulation.[15] In the SSFLC geometry the smectic layers form a chevron structure, as depicted in Fig. 1.[16] This results in a twisted director profile through the thickness of the device when no field is applied.[17,18] In the current paper a detailed study has been carried out on the effect of the SSFLC internal structure and on the optimization of the diffraction efficiency for SSFLC-geometry phase-modulation structures. Diffraction efficiencies are properly calculated by use of a vector beam propagation method[19] (VBPM) suitable for liquid-crystal (LC)-device calculations.[20] This method provides a wide-angle forward-only numerical solution to Maxwell's equations and correctly in-

C. V. Brown (carl.brown@eng.ox.ac.uk) and E. E. Kriegis are with the Department of Engineering Science, University of Oxford, Parks Road, Oxford OX1 3PJ, United Kingdom. E. E. Kriezis is also with the Department of Electrical and Computer Engineering, Aristotle University of Thessaloniki, Thessaloniki GR-54124, Greece.

Received 17 September 2002; revised manuscript received 8 January 2003.

0003-6935/03/132257-07$15.00/0

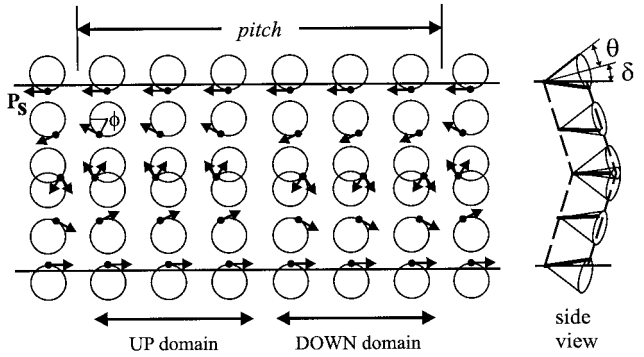

Fig. 1. Illustration of the FLC diffraction grating geometry.

corporates the optical anisotropy effects presented by the LC layer. The incoming wave front is propagated through the anisotropic material in small axial steps; the axial, as well as the lateral (transverse), variation of the LC director orientation is taken into consideration. Such an approach provides accurate and realistic calculations for the LC optics in two dimensions and does not suffer from the restrictions of the traditional one-dimensional methods for LC optics (Jones calculus or Berreman method). The influence of an externally applied ac field and the role of the material spontaneous polarization on the diffraction efficiency of SSFLC phase gratings are thoroughly quantified.

2. Diffraction Efficiency and Polarization Independence

To calculate the optimum diffraction efficiency of a SSFLC device, we will consider a linear array of pixels in which the optical state of the pixels alternates between the up and the down switched states. The so-called C2U geometry for a SSFLC is depicted in Fig. 1 where the arrows show the direction of the spontaneous polarization as a function of distance through the layer. The FLC director lies at a rotation angle $\phi(z)$ around the smectic cone of half-angle θ, and the two arms of the layer chevron are orientated at angles of $\pm\delta$. If there are no applied fields, the FLC profile is in the relaxed state in which the twist of the FLC director varies roughly linearly from its position at the bottom (top) of the cone at the upper (lower) surface to one of the bistable orientations of maximum twist at the chevron interface positioned at the center of the cell. This structure has been referred to as a twisted director profile (TDP).[17]

In the approach of Warr and Mears,[7] the fraction of the incident light intensity that is diffracted out of the zero-order on-axis spot, termed here as total diffraction efficiency η_{TOT}, was calculated with the following expression:

$$\eta_{TOT} = \frac{|\mathbf{E}_{inc}|^2 - \frac{1}{4}|\mathbf{E}_1 + \mathbf{E}_2|^2}{|\mathbf{E}_{inc}|^2}. \quad (1)$$

Here the electric field vector, or Jones vector, of the normally incident light is given by $\mathbf{E}_{inc}$. The vectors $\mathbf{E}_1$ and $\mathbf{E}_2$ are the two possible electric field vectors that result after transmission of the incident field through the SSFLC device. The vector $\mathbf{E}_1$ describes the electric field after transmission through a pixel that has an optical axis that is oriented at an azimuthal angle $+\beta$ in the plane of the SSFLC device. The vector $\mathbf{E}_2$ results after transmission through a pixel that has an optical axis that is oriented at the azimuthal angle $-\beta$. It was shown in Ref. 7 that, if the pixels can be described as uniform birefringent slabs, the value of the fraction η_{TOT} is totally independent of the polarization orientation of the incident electric field vector $\mathbf{E}_{inc}$, and it is equal to $\eta_{TOT} = \sin^2(2\beta)\sin^2(\pi d\Delta n/\lambda)$. This result was generalized to the case of a two-dimensional rectangular array of pixels that are as likely to be in the optical state $+\beta$ as in the other state $-\beta$. For the above analysis to be valid, pixels should be substantially larger compared with the light wavelength in order to justify an independent treatment of the two states. However, a more serious limitation on the size of the pixels is that the lateral dimension must be several times greater than the thickness of the FLC layer. This is to avoid the influence of pixel-edge effects, including the finite width of the domain boundary between pixels with different orientations of the optical axis. In a typical SSFLC device with thickness around 1–2 μm, the optical effect of the domain boundary will occur over a lateral width that is also of the order of 1–2 μm, and so the use of Eq. (1) is justified for pixel sizes around 10–20 μm. Furthermore, Eq. (1) gives no explicit information on the first-order diffraction efficiency, although in many cases it is this latter efficiency that is of interest.

It is proved here that this polarization independence will be true for any wave plate that can be described in terms of a unitary Jones matrix for a linear array of pixels in which the optical axis orientation alternates between a positive twist angle and a negative twist angle in adjacent pixels. This can be demonstrated by the substitution into Eq. (1) of the expressions for $\mathbf{E}_1$ and $\mathbf{E}_2$ below in Eqs. (2), where the general unitary Jones matrices for a positive rotation and a negative rotation of the optic axis are given by $\mathbf{J}_1$ and $\mathbf{J}_2$.[16]

$$\mathbf{E}_1 = \mathbf{J}_1\mathbf{E}_{inc} = \begin{bmatrix} a & b \\ -b^* & a \end{bmatrix}\mathbf{E}_{inc}, \quad (2a)$$

$$\mathbf{E}_2 = \mathbf{J}_2\mathbf{E}_{inc} = \begin{bmatrix} a & -b \\ b^* & a \end{bmatrix}\mathbf{E}_{inc}. \quad (2b)$$

This gives the result that $\eta_{TOT} = 1 - aa^*$ for any input electric field vector. The polarization independence of the diffraction efficiency η_{TOT} will therefore hold for the case of an array of SSFLC pixels that alternate between the up and the down states, as shown in Fig. 1. In this case the sign of the twist profile changes, but the tilt profile is the same for the two states, and so the Jones matrices will be of the same form as those shown in Eqs. (2). This can readily be demonstrated for a TDP by examination of

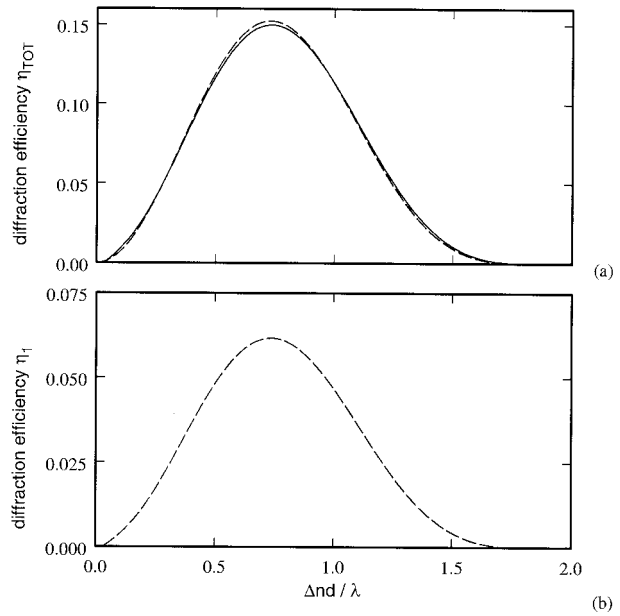

Fig. 2. Diffraction efficiencies as a function of the parameter $\Delta nd/\lambda$ for the diffraction geometry in Fig. 1: (a) total diffraction efficiency (η_{TOT}), with the dashed curve corresponding to the Jones calculus and the solid curve corresponding to the VBPM, and (b) first-order diffraction efficiency (η_1) calculated by the VBPM.

the analytical form of the appropriate Jones matrix.[17] It should be noted that the result would be independent of the pitch p (and the pixel size) as long as they are substantially larger than the optical wavelength—thus justifying the above simple treatment based on Jones matrices—and the effect of any domain walls between up and down states can be neglected.[21]

3. Diffraction from the Relaxed Surface-Stabilized Ferroelectric Liquid-Crystal Structure

In Fig. 2(a) the value of the total diffraction efficiency (η_{TOT}) is shown as a function of the dimensionless parameter $\Delta nd/\lambda$ for the TDP structure shown in Fig. 1. The dashed curve was derived by use of the Jones calculus[18] for different cell thicknesses at $\lambda = 632.8$ nm together with the refractive-index values given in Table 1. The solid curve in Fig. 2(a) also shows the value of η_{TOT} obtained with a rigorous VBPM for LC devices,[20] and Fig. 2(b) shows the VBPM prediction for the first-order diffraction efficiency (η_1). VBPM calculations have been performed considering a pixel size of 30 μm (pitch equal to 60 μm) and a sharp transition between the two FLC states. Curves of Fig. 2(a) are in excellent agreement, whereas the η_1 curve of Fig. 2(b) shows a shape and position of the maximum similar to those of Fig. 2(a), but the corresponding values are now lower as they account only for the first-order diffracted light. Clearly, the first-order diffraction efficiencies available with such TDP profiles are significantly lower compared with the theoretical maximum first-order efficiency of $4/\pi^2 = 40.5\%$ for a square-profile grating made of a high-cone-angle (45°) material with a half-wave-plate thickness. As mentioned above in the VBPM simulations, we have used a two-dimensional director profile with a sharp transition between the two FLC states; this eventually sets an idealistic domain-wall thickness equal to the lateral discretization step, δx, used (here a value of $\delta x = 50$ nm has been used). It is expected that there will be further reductions in the diffraction efficiencies when walls of a realistic size are fully taken into account. The greatest reduction will occur for small-sized pixels. This effect is under investigation and will be reported in a future publication.

Table 1. LC Material Parameters Used throughout the Simulations

Parameter	Numerical Value
Elastic constant B	5.7 pN
Permittivity ε_1	5.09
Dielectric biaxiality $\partial\varepsilon$	0.67
Dielectric anisotropy $\Delta\varepsilon$	−1.60
Smectic cone angle θ	26.0°
Layer tilt angle δ	21.1°
Refractive index n_o	1.6317
Refractive index n_e	1.4789

The curves in Fig. 2 exhibit a maximum at $\Delta nd/\lambda = 0.74$, which lies between the half-wave-plate condition, $\Delta nd = \lambda/2$, and the full-wave-plate condition, $\Delta nd = \lambda$. The position at which this maximum occurs can be interpreted in terms of two competing effects. The optical properties of a TDP can be approximately described by an average angle of the optical axis β_{EXT} that varies with the parameter $\Delta nd/\lambda$ and the magnitude of the total twist through the layer.[17] The value of β_{EXT} diverges toward a maximum of 45°, which is close to the full-wave-plate condition, which tends to increase the diffraction efficiency. However, as the value of $\Delta nd/\lambda$ approaches this condition, both phase shifts of the vectors $\mathbf{E}_1$ and $\mathbf{E}_2$ relative to the input electric field vector $\mathbf{E}_{inc}$ tend to π rads. The relative phase shift between neighboring pixels therefore tends to zero, which acts to reduce the diffraction efficiency.

4. Diffraction from ac-Stabilized Ferroelectric Liquid-Crystal Structures

In Fig. 3(a) and 3(b) twist and tilt profiles have been calculated across the width of the SSFLC layer as a function of an applied ac voltage, which is varied from 0 V_{ac} (dashed curve) to 16 V_{ac} in increments of 2 V_{ac}. The profiles were calculated with the methods described in an earlier publication[22] that used the measured parameters for the LC material SCE8* given in Table 1. The highest voltage was chosen to be 16 V_{ac} because this is a typical magnitude at which the onset of nonreversible voltage-induced layer deformations will occur in a SSFLC device. It is implicit in the calculations that the ac voltage is applied at a frequency that is too high to couple to the spontaneous polarization, so that the domain widths are static and no switching occurs between bistable states. For SCE8* at room temperature, this frequency would be

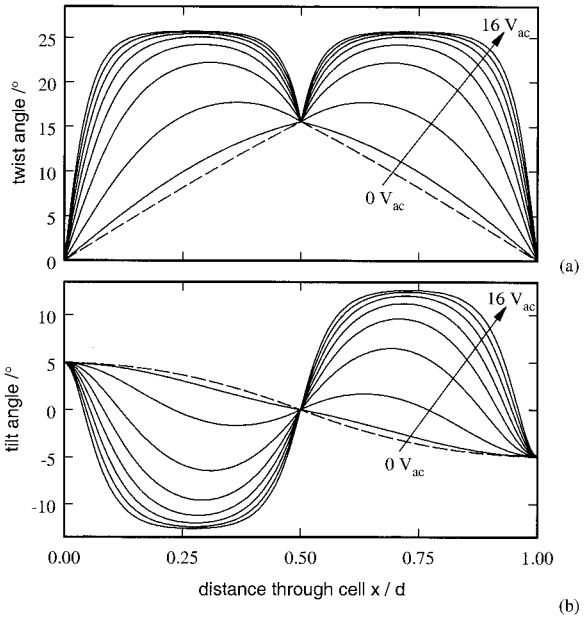

Fig. 3. Twist and tilt profiles as a function of distance through the FLC layer. Curves are shown for zero-applied voltage (dashed curve) and for applied ac voltages from 2 to 16 V_{ac} in steps of 2 V_{ac} (solid curves).

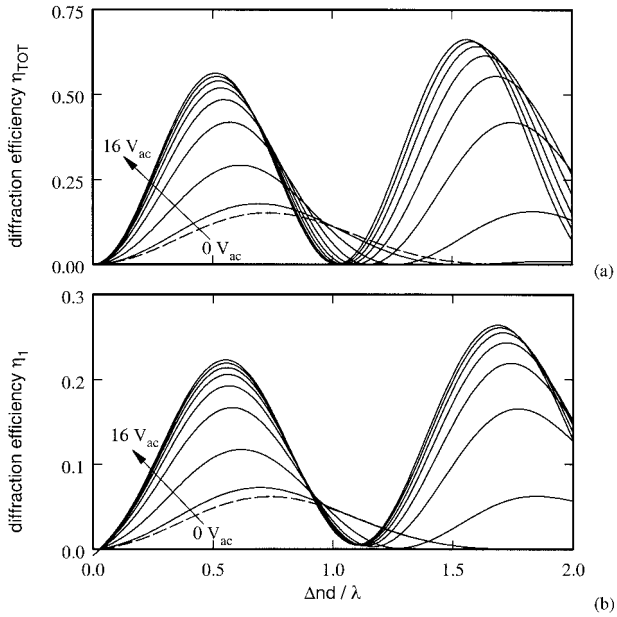

Fig. 4. Diffraction efficiencies as a function of the parameter $\Delta nd/\lambda$ for the twist and tilt profiles of Fig. 3: (a) total diffraction efficiency (η_{TOT}) obtained by the Jones calculus and (b) first-order diffraction efficiency (η_1) obtained by the VBPM.

in the range of 10–20 kHz.[23] In this case, both the up and the down domains are similarly distorted, but the twist profiles have opposite signs. The profiles become increasingly distorted toward larger twist angles as the ac voltage is increased. At the highest voltage, both the twist and the tilt show a saturation effect in which the profile flattens, and there is an increased proportion of the cell lying uniformly at the maximum angle. This effect is known as ac stabilization; as the voltage tends to infinity, the azimuthal angle ϕ describing the FLC orientation tends to a constant value whose magnitude is determined by the angles δ and θ and the values of the biaxial permittivities ε_1, $\partial\varepsilon$, and $\Delta\varepsilon$.[24] For the parameters used in the simulation, the maximum value of the twist is 25.8°, and the maximum value of the tilt is 12.8°.

The diffraction efficiency for the profiles of Fig. 3 is plotted as a function of $\Delta nd/\lambda$ in Fig. 4. Figure 4(a) shows the total diffraction efficiency η_{TOT} calculated by use of the Jones calculus and Eq. (1). Figure 4(b) shows the first-order diffraction efficiency η_1 calculated by use of the VBPM and 30-μm pixel size. It should be emphasized that each of the curves in Fig. 4(a) and 4(b) corresponds to one of the profiles shown in Fig. 3(a) and 3(b). If the value of $\Delta nd/\lambda$ is adjusted when the cell thickness d is changed, then a different voltage value would be required to achieve the same profile at different values of d.

As seen in Fig. 4(a), when the ac voltage is increased, the position of the maximum at $\Delta nd/\lambda = 0.74$ decreases until, at 16 V_{ac}, it is close to the half-wave-plate condition at $\Delta nd = \lambda/2$. This is a result of the fact that the tilt and twist profiles are becoming more uniform through the cell thickness as the voltage increases, making the device behave as a sequence of oppositely switched uniform wave plates. Accompanying this shift in the maximum is an increase in the value of the maximum diffraction efficiency. This occurs because the average twist angle also increases with increased applied voltage. The change is less marked at the higher voltage because of the saturation effect. The same comments apply to η_1, as demonstrated in Fig. 4(b), and the shape of these curves is similar to those of Fig. 4(a). It should be noted that the maxima and minima in Fig. 4(b), especially for the higher-voltage curves, are occurring at higher $\Delta nd/\lambda$ values as compared with those of Fig. 4(a). This is due to the fact that the Jones calculus is not properly treating the tilt, resulting in higher error for increased values of voltage (and therefore tilt). In contrast, the VBPM rigorously accounts for this tilt effect.

5. Diffraction from Ferroelectric Liquid Crystal Structures with a High Spontaneous Polarization

In Figs. 5(a) and 5(b), twist and tilt profiles have been calculated across the width of the SSFLC layer as a function of the magnitude of the spontaneous polarization P_s of the FLC material for the case in which there is no externally applied voltage. The same calculation method was used for the profiles in Fig. 3, but the effect of the self-interaction of the polarization through the structure has now been included, following the approach detailed in Ref. 25. For the profiles shown in Fig. 5, the polarization varies from 0 (dashed curve) to 25 nC/cm^2 in increments of 5 nC/cm^2. This range spans the values found in some commercial low-cone-angle ferroelectric materials,

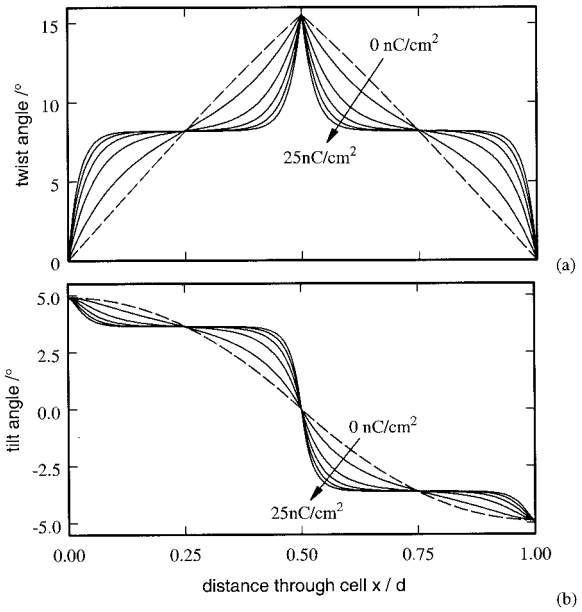

Fig. 5. Twist and tilt profiles as a function of distance through the FLC layer. Curves are shown for zero spontaneous polarization (dashed curve) and for the values 5, 10, 15, 20, and 25 nC/cm^2.

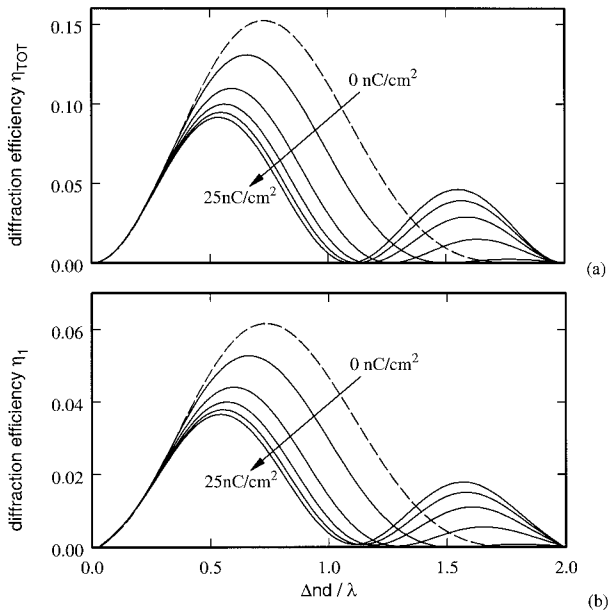

Fig. 6. Diffraction efficiencies as a function of the parameter $\Delta nd/\lambda$ for the twist and tilt profiles of Fig. 5: (a) total diffraction efficiency (η_{TOT}) obtained by the Jones calculus and (b) first-order diffraction efficiency (η_1) obtained by the VBPM.

SCE8* and SCE13*,[26] intended for use in the SSFLC mode; at room temperature $P_s \approx 6.5$ nC/cm^2 for SCE8* and $P_s \approx 26.0$ nC/cm^2 for SCE13*.

As the magnitude of P_s is increased, the self-interaction effect tends to line up the orientation of the polarizations across the width of the layer. Acting against this polarization torque is an elastic torque whose magnitude is determined by the value of the constant B in Table 1. This elastically couples the director orientation in the bulk of the FLC material to the pinned director orientations at the surfaces and at the chevron cusp in the center of the cell. At the higher values of P_s, the self-interaction effect wins out, and so an increasing fraction of the structure is oriented at values of the twist and tilt angles that are independent of position and lie midway between the surface and the chevron positions.

The diffraction efficiency for the profiles of Fig. 5 is plotted as a function of $\Delta nd/\lambda$ in Fig. 6, where Fig. 6(a) shows values of η_{TOT} calculated with the Jones calculus and Eq. (1) and Fig. 6(b) shows values of η_1 calculated with the VBPM technique. As before, each of the curves in Fig. 6 corresponds to one of the profiles shown in Fig. 5, and the shape of the curves in Fig. 6(a) for η_{TOT} and in Fig. 6(b) for η_1 are similar, apart from the difference in magnitude. In this set of profiles the maxima and minima of Fig. 6(b) closely coincide with those of Fig. 6(a) as the associated tilt values are now lower compared with those of Section 4, and therefore the error suffered by the Jones calculus is expected to be smaller. As the value of P_s is increased, the position of the maximum at $\Delta nd/\lambda = 0.74$ shifts toward the half-wave-plate condition as the tilt and twist profiles become more uniform through the cell thickness. However, accompanying this shift in the maximum, there is now a decrease in the value of the maximum diffraction efficiency as a higher proportion of the cell becomes oriented at the lower twist angle of 7.8°.

Although the highest value of P_s that was used in the simulation is available in a commercial SSFLC mixture, the director profile through the layer is likely to depart from the idealized profiles shown, particularly for the higher values of P_s. There are two effects that must be considered. First, owing to the polarity of the molecules in FLC materials, they normally contain ionic contamination at levels that are higher than similar nematic formulations. It has been suggested that the presence of these ionic species screens out some of the polarization self-interaction effects, which would smooth out the rapid changes in the profiles shown in Fig. 5.[27–29] Therefore the actual profile for a given value of P_s would actually resemble one for which P_s was much lower. Second, at high values of P_s it has been reported that a polar interaction at the surfaces becomes significant. In this case the director would not lie parallel to the surfaces, as shown in Fig. 1, but would, in fact, lie at an angle determined by the balance of the bulk elastic and polarization torques and the polar surface interaction energy.[30] This balance leads to the possibility of splayed director profile states in which the symmetry between the top and the bottom halves of the cell is broken. In the C2 SSFLC alignment geometry considered in this paper, this asymmetry is usually small. However, in the C1 alignment geometry, this asymmetry can be much larger.

6. Discussion

In this paper the effect of the spontaneous polarization and the applied ac fields have been treated separately. Total and first-order diffraction efficiencies have been calculated for realistic sets of ac stabilization voltages and spontaneous polarization magnitudes. It has been concluded that maximum diffraction efficiencies are occurring at a value of $\Delta nd/\lambda$ between 0.5 and 1.0, strongly dependent on the particular director profile and, as a consequence, the applied ac voltage or the spontaneous polarization magnitude. This is important as it is usually thought that a half-wave-plate condition should lead to maximum diffraction efficiency—this is only true in the case of alternating oppositely switched uniform wave plates. It has also been shown by our calculations that the ac stabilization technique substantially improves the device's diffraction efficiency. In an even more realistic approach, the profiles shown in Fig. 3 might have to be further modified because there will be a self-interaction effect of the P_s as well as a coupling to the applied ac field.

All the calculated curves showing the diffraction efficiencies η_{TOT} and η_1 in Figs. 2, 4, and 6 are independent of the orientation of the input polarization. For the SSFLC device that has been investigated, this polarization insensitivity is a consequence of the fact that the twist profiles in adjacent pixels are alternating in sign, whilst the tilt profiles remain constant and do not change, and it will be true only for pixels substantially larger than the optical wavelength with sharp transitions between the two FLC states. Of course, other possible polarization-insensitive devices can be found, for instance, devices based on the opposite extreme of very small-sized (subwavelength) LC structures, where the above limitation would not apply.[31,32]

The domain walls that occur between the up and the down regions have not been considered in this paper. For small pitches the presence of domain walls introduces a dependence on the orientation of the input polarization and also reduces the diffraction efficiency. For a device thickness of the order $d = 2$ μm, a preliminary analysis shows that this effect becomes significant when the pixel size is reduced to the order of 5 μm, justifying the assumptions made in Section 2. A more detailed examination of this dependence will be presented in a future publication.

We gratefully acknowledge the useful contributions made by T. D. Wilkinson, I. G. Manolis, and W. A. Crossland from the Department of Engineering Science, University of Cambridge, during the preparation of this paper.

References and Notes

1. R. M. Turner, D. A. Jared, G. D. Sharp, and K. M. Johnson, "Optical correlator using very-large-scale integrated circuit/ferroelectric-liquid-crystal electrically addressed spatial light modulators," Appl. Opt. **32,** 3094–3101 (1993).
2. T. D. Wilkinson, Y. Petillot, R. J. Mears, and J. L. de Bougrenet de la Tocnaye, "Scale-invariant optical correlators using ferroelectric liquid-crystal spatial light modulators," Appl. Opt. **34,** 1885–1890 (1995).
3. S. E. Broomfield, M. A. Neil, and E. G. Paige, "Programmable multiple-level phase modulation that uses ferroelectric liquid-crystal spatial light modulators," Appl. Opt. **34,** 6652–6665 (1995).
4. R. J. Mears, W. A. Crossland, M. P. Dames, J. R. Collington, M. C. Parker, S. T. Warr, T. D. Wilkinson, and A. B. Davey, "Telecommunications applications of ferroelectric liquid-crystal smart pixels," IEEE J. Sel. Top. Quantum Electron. **2,** 35–46 (1996).
5. W. A. Crossland, I. G. Manolis, M. M. Redmond, K. L. Tan, T. D. Wilkinson, M. J. Holmes, T. R. Parker, H. H. Chu, J. Croucher, V. A. Handerek, S. T. Warr, B. Robertson, I. G. Bonas, R. Franklin, C. Stace, H. J. White, R. A. Woolley, and G. Henshal, "Holographic switching: the ROSES demonstrator," J. Lightwave Technol. **18,** 1845–1854 (2000).
6. C. W. Slinger, R. W. Bannister, C. D. Cameron, S. D. Coomber, I. Cresswell, P. M. Hallett, J. R. Hughes, V. C. Hui, J. C. Jones, R. Miller, V. Minter, D. A. Pain, D. C. Scattergood, D. T. Sheerin, M. J. Smith, and M. Stanley, "Progress and prospects for practical electroholographic display systems," in *Practical Holography XV and Holographic Materials VII*, S. A. Benton, S. H. Sylvia, and T. J. Trout, eds., Proc. SPIE **4296,** 18–32 (2001).
7. S. Warr and R. Mears, "Polarization-insensitive operation of ferroelectric liquid crystal devices," Electron. Lett. **31,** 714–716 (1995).
8. S. Warr and R. Mears, "Polarisation insensitive diffractive FLC systems," Ferroelectrics **181,** 53–59 (1996).
9. S. E. Broomfield, M. A. Neil, E. G. Paige, and G. G. Yang, "Programmable binary phase-only device based on ferroelectric liquid crystal SLM," Electron. Lett. **28,** 26–28 (1992).
10. J. S. Patel and J. W. Goodby, "Alignment of liquid crystals which exhibit cholesteric to smectic* phase transitions," J. Appl. Phys. **59,** 2355–2360 (1986).
11. CS2005 is the trade name for a commercial high-tilt ferroelectric LC material available from Lixon Department, CHISSO Corporation, Chuo-ku, Tokyo, Japan.
12. J. Newton, H. Coles, P. Hodge, and J. Hannington, "Synthesis and properties of low-molar-mass liquid-crystalline siloxane derivatives," J. Mater. Chem. **4,** 869–874 (1994).
13. N. A. Clark and S. T. Lagerwall, "Sub-millisecond bistable electro-optic switching in liquid crystals," Appl. Phys. Lett. **36,** 899–901 (1980).
14. D. C. O'Brien, R. J. Mears, T. D. Wilkinson, and W. A. Crossland, "Dynamic holographic interconnects that use ferroelectric spatial light modulators," Appl. Opt. **33,** 2795–2803 (1994).
15. J. C. Jones, M. J. Towler, and J. R. Hughes, "Fast, high contrast ferroelectric liquid crystal displays and the role of dielectric biaxiality," Displays **14,** 86–93 (1993).
16. N. A. Clark and T. P. Reiker, "Smectic C chevron, a planar liquid-crystal defect—implications for the surface stabilized ferroelectric liquid crystal geometry," Phys. Rev. A **37,** 1053–1056 (1988).
17. M. H. Anderson, J. C. Jones, E. P. Raynes, and M. J. Towler, "Optical studies of thin layers of smectic C materials," J. Phys. D **24,** 338–342 (1991).
18. E. P. Raynes and R. J. Tough, "The guiding of plane polarized-light by twisted liquid-crystal layers," Mol. Cryst. Liq. Cryst. **2,** 139–145 (1985).
19. C. L. Xu, W. P. Huang, J. Chrostowski, and S. K. Chaudhuri, "A full-vectorial beam propagation method for anisotropic waveguides," J. Lightwave Technol. **12,** 1926–1931 (1994).
20. E. E. Kriezis and S. J. Elston, "Wide-angle beam propagation method for liquid-crystal device calculations," Appl. Opt. **39,** 5707–5714 (2000).

21. J. Z. Xue and N. A. Clark, "Stroboscopic microscopy of ferroelectric liquid crystals," Phys. Rev. E **48,** 2043–2054 (1993).
22. C. V. Brown and J. C. Jones, "Accurate determination of the temperature- and frequency-dependent smectic C biaxial permittivity tensor," J. Appl. Phys. **86,** 3333–3341 (1999).
23. C. V. Brown, J. C. Jones, and M. S. Bancroft, "Detailed simulation of the Goldstone mode response of FLCs in the surface stabilized geometry," Ferroelectrics **245,** 743–751 (2000).
24. J. C. Jones, E. P. Raynes, M. J. Towler, and J. R. Sambles, "Dielectric biaxiality in smectic C host systems," Mol. Cryst. Liq. Cryst. **199,** 277–285 (1991).
25. M. J. Towler, J. R. Hughes, and F. C. Saunders, "Switching behavior of smectic C* liquid crystals," Ferroelectrics **113,** 453–465 (1991).
26. SCE8* and SCE13* are the trade names for pitch-compensated, low-tilt commercial ferroelectric LC mixtures developed by BDH Ltd., Poole, Dorset, UK.
27. M. H. Lu, K. A. Grandall, and C. Rosemblatt, "Polarization induced renormalization of the B(1) elastic modulus in a ferroelectric liquid-crystal," Phys. Rev. Lett. **68,** 3575–3578 (1992).
28. K. Okano, "Electrostatic contribution to the distortion free-energy density of ferroelectric liquid crystals," Jpn. J. Appl. Phys. **25,** 846–847 (1986).
29. D. C. Ulrich, "Domain formation and switching in ferroelectric liquid crystals," Ph.D. dissertation (University of Oxford, Oxford, UK., 1995).
30. J. E. Maclennan, N. A. Clark, M. J. Handschy, and M. R. Meadows, "Director orientation in chevron surface-stabilized ferroelectric liquid crystal cells," Liq. Cryst. **7,** 753–785 (1990).
31. R. Blacker, K. Lewis, I. Mason, I. Sage, and C. Webb, "Nanophase polymer dispersed liquid crystals," Mol. Cryst. Liq. Cryst. **329,** 799–810 (1999).
32. T. Vallius, P. Vahimaa, J. Turunen, and Y. Svirko, "Polarization diffractive optics of chiral nanogratings," in *Proceedings of International Quantum Electronics Conference*, Moscow, Russia (2002).